Indian Journal of Chemical Technology
Vol. 24, March 2017, pp. 123-133

# Kinetic and thermodynamic study of Am(III) sorption on Na-bentonite: Comparison of linear and non-linear methods

Tao Yu *,[1,2] , Shimin Liang[2] & Xiaoqi Shang[2]

[1]State Key Laboratory Breeding Base of Nuclear Resources and Environment, East China Institute of Technology, Nanchang, 330013, Jiangxi, China

[2]School of Nuclear Engineering and Geophysics, East China Institute of Technology, Nanchang, 330013, Jiangxi, China

E-mail: xiaoshan770@163.com

*Received 7 September 2015; accepted 30 June 2016*

Kinetic and thermodynamic studies of Am (III) sorption on Na-bentonite have been investigated under the given conditions. Comparisons of linear and non-linear methods of three kinetic rate equations and four thermodynamic isotherms have been tested on the experimental data. The results show that sorption of Am (III) on Na-bentonite can be represented by a pseudo-second-order rate equation, and the non-linear pseudo-second-order kinetic expression could fit the kinetics better. The thermodynamic parameters ($\Delta H^0$, $\Delta S^0$ and $\Delta G^0$) of Am (III) sorption on Na-bentonite indicate that the sorption process was spontaneous. Freundlich isotherm model is the best-fit model to the experimental data for the sorption of Am (III) on Na-bentonite. Furthermore, the non-linear method is a better way to describe the sorption isotherm than the linear method. Non-linear methods are found to be the better way to obtain the kinetic and thermodynamic parameters.

**Keywords:** Sorption, Am (III), Kinetic, Thermodynamics, Linear and non-linear methods

Study on the safety disposal of nuclear waste has been an important project since the widely use of nuclear energy, and the high-level radioactive waste sorption on different adsorbents becomes an indispensable content of the study[1,2]. $^{241}$Am and bentonite are the representative adsorbate and adsorbent in these researches. Bentonite has been used as a barrier material for landfills and final repositories of hazardous waste, and widely studied in nuclear waste management because of its strong sorption ability and low permeability[3,4]. Bentonite has been found to have a large BET surface area and high cation exchange capacity, good heat conductivity and high swelling property, compared with other absorbents[5,6]. $^{241}$Americium is an actinide isotope having a large number of applications[7,8]. As one of strategic elements of the nuclear fuel cycle, the sorption and migration of Am (III) on bentonite are becoming an important research direction.

In many previous sorption studies, linear regression is frequently used to describe the process of sorption kinetics and determine the best-fitting isotherm[9-11]. Well, the results of further research show that, non-linear method is a better way to describe kinetic process and obtain isotherm parameters[12,13].

In our previous work, some similar experiments of Am (III) sorption on Na-bentonite were carried out by linear and batch method[14]. Sorption of Am (III) on Na-bentonite is strongly dependent on *p*H values and ionic strength. The results showed that the sorption increases with increasing *p*H values at *p*H <7, and then maintains a high level at *p*H >7. The sorption of Am (III) on bentonite is quickly to achieve the sorption equilibration, and the time to achieve the sorption equilibrium was about 4 h. The presence of HA enhances the sorption of Am (III) on Na-bentonite at low *p*H values, and reduces the sorption at high *p*H values, while there was a valley at *p*H 7～7.5. The sorption of Am (III) on Na-bentonite is an endothermic and spontaneous process, indicated by the thermodynamic parameters. The physicochemical behaviour of Am (III) is dominated by many factors, such as the nature of bentonite, humic substances, *p*H, ionic strength, temperature, etc. The sorption isotherms of Am (III) on Na-bentonite could be described by linear Freundlich model.

In this work, the linear and non-linear method of three kinetic rate equations (pseudo-first-order, pseudo-second-order and ‘pseudo-n-order’ kinetic expression) and four isotherms (Langmuir, Freundlich, sips and Toth) were tried to compare in experiment examining of Am (III) sorption on Na-bentonite. The Chi-square tests were used as an error function assessment to evaluate the fit of the equations to the experimental results.

## Experimental Section

### Materials

Materials and reagents used in the experiments were analytical grade. Bentonite was achieved from Gaomiaozi County (Inner Mongolia, China) and converted into Na-bentonite[15]. Chemical components of Na-bentonite analyzed by X-ray fluorescence diffraction were: $SiO_2$ 85.11%, $Al_2O_3$ 12.37%, $Fe_2O_3$ 3.01%, MgO 1.75%, $Na_2O$ 1.37%, $K_2O$ 0.38%, CaO 0.24%. The $^{241}$Am stock solution was provided by Institute of Modern Physics (Chinese Academy of Sciences), and the initial concentration of Am(III) solution was $3.6\times10^{-9}$ mol/L. A HPGe detector was used to determine the $\gamma$-spectra of $^{241}$Am stock solution. Humic acid was extracted from the soil of Lintan County (Gansu Province)[16].

The surface properties of bentonite were characterized by X-ray diffraction (XRD) and Scanning Electron Microscope (SEM). XRD analysis was performed with Cu $K\alpha$ radiation ($\lambda$=0.15406 nm) with a Rigaku diffractometer. The operation conditions of XRD were 40 kV and 80 mA. The $2\theta$ rate was 100-800. Patterns were identified by comparison to the JCPD standards. The morphology of Na-bentonite samples were studied by scanning electron microscopy at 30 kV.

### Sorption experiments

The sorption experiments of Am (III) on Na-bentonite (0.025-0.5g/L) were carried out under three different temperatures: 298.15K, 318.15K and 338.15K. The stock suspension of Na-bentonite, and the stock solution of NaCl and Am (III) were added into the polyethylene tubes to achieve the desired concentrations. The solid and liquid phases were separated by centrifugation at 12,000 rpm for 30min after the suspensions were shaken for 12 h. The $\gamma$-activities of solution aliquots and solid aliquots were measured using a counter with a NaI detector. The experiments of the study were all carried out under the normal conditions.

The sorption percentage and the distribution coefficient ($K_d$) were calculated by the following equations:

$$\text{Sorption\%} - \frac{(n-n_0)-(n_1-n_0)}{(n-n_0)}\times 100 \qquad \ldots (1)$$

$$K_d = C_s / C_{eq} \qquad \ldots (2)$$

where $n$, $n_0$, $n_1$ are the count of Am (III) solution, background of the counter and liquid phases, respectively, $Cs$ is the concentration of Am(III) on solid phase (mol/g), $Ceq$ is the concentration of Am (III) in liquid phase (mol/L).

### Sorption kinetic models

There are two frequently used expressions to describe and predict the sorption kinetics: the pseudo-first-order and pseudo-second-order rate equation. The pseudo-first-order rate equation is given by the following equation [17]:

$$dq/dt = K_1(q_e - q_l) \qquad \ldots (3)$$

where $K_1$ ($h^{-1}$) is the pseudo-first-order rate constant of sorption, $q_t$ (mg/g of dry weight) is the amount of Am (III) adsorbed on the surface of Na-bentonite at time t (h), and $q_e$(mg/g) is the calculated sorption capacity at equilibrium time. Integrating and applying boundary conditions $t$=0 to $t=t$ and $q_t$=0 to $q_t=q_t$, Equation (3) can be rearranged to obtain a linear and a non-linear form [18]:

$$\ln(q_e - q_t) = 1n q_e - K_1 t \qquad \ldots (4)$$

$$q_t = q_e(1 - e^{-K1t}) \qquad \ldots (5)$$

The pseudo-second-order kinetics model is further used to analyze the kinetic data, which can be written as:

$$d_q / d_t = K_2 (q_e - q_t)^2 \qquad \ldots (6)$$

where $K_2$ (g $mg^{-1}$ $h^{-1}$) is the pseudo-second-order rate constant of sorption, integrating this for the boundary conditions t=0 to t=t and $q_t$=0 to $q_t$=$q_t$, gives the linear and non-linear forms [19]:

$$\frac{t}{ql} = \frac{1}{K_2 q_e^2} + \frac{1}{q_e} t \qquad \ldots (7)$$

$$qt = \frac{K_2 q_e^2}{1 + K_2 q_e t} \qquad \ldots (8)$$

Combining with the derivation process above, we could derive a general kinetic model:

$$dq/dt = K_n (q_e - q_t)^n \qquad \ldots (9)$$

Derivative this equation:

$$\int \frac{dq_t}{(q_e - q_t)^n} = \int K_n dt \qquad \ldots (10)$$

Being n>1, and the boundary conditions t=0 to t=t and $q_t$=0 to $q_t$=$q_t$:

$$\int_0^{qt} -\frac{d(q_e - q_t)}{(q_e - q_t)^n} = \int_0^t K_n dt \qquad \ldots (11)$$

The integration of equation (11):

$$(n-1)^{-1}(q_e-q_t)^{-(n-1)}=K_nt+C \qquad \ldots (12)$$

Where C is a constant, under the boundary conditions t=0 to t=t and $q_t$=0 to $q_t$=$q_t$,

$$C=(n-1)^{-1}\,q_e^{-(n-1)} \qquad \ldots (13)$$

Thus the sorption kinetic equation can be formulated as:

$$(n-1)^{-1}(q_e-q_t)^{-(n-1)}=K_nt+(n-1)^{-1}q_e^{-(n-1)} \qquad \ldots (14)$$

and the nonlinear model:

$$q_t=q_e-\frac{q_e}{\left[1+(n-1)K_nq_e^{(n-1)}t\ \right]^{\frac{1}{(n-1)}}} \qquad \ldots (15)$$

Equation (15) could be named as 'pseudo-n-order' where $K_n$ ($g^{(n-1)}$ $mg^{-(n-1)}$ $h^{-1}$) is the rate constant of sorption. While, there are at least four linear forms of pseudo-second-order kinetics, and the different linearized forms of the pseudo-first-order and pseudo-second-order equations are given in Table 1.

The chi-square ($x^2$) tests are used as an error function assessment to evaluate the fit of the equations to the experimental results[20, 21]

$$x^2=\sum\frac{(q_e^t-q_e)^2}{q_e} \qquad \ldots (16)$$

where $q_e$' (mg/g) and $q_e$ (mg/g) are the measured($q_t$) and calculated sorption capacity at equilibrium time.

The diffusion model was used to simulate the experimental data[22]:

$$Bt=-In(1-F)-0.4977 \qquad \ldots (17)$$

where $F=q_t\ /q_e$, $B=\pi^2D_i\ /d^2$, $D_i$ is the diffusion coefficient, $d$ is the particle radius.

Weber-Morris intraparticle diffusion model can describe the process of diffusion further, and the model is described as follows [23]:

$$q_t=k_pt^{0.5}+C \qquad \ldots (18)$$

where $k_p$ (kg/(mg $h^{0.5}$)) is the intraparticle diffusion rate constant and C is the intercept. The $k_p$ values can be evaluated from the slope of the linear plot of $q_t$ versus $t^{0.5}$. The values of C give an idea about the thickness of the boundary layer.

## Results and Discussion

### Characterization

SEM micrographs of raw bentonite(a) and Na-bentonite(b) are shown in Fig. 1. From Fig. 1, as can be seen that raw bentonite and exhibits a layer structure and some pieces pile up and form ridge, and the size of a certain single piece is about 0.5~3μm in width. Compared with raw bentonite, the structure of Na-bentonite is not changed obviously, while the latter surface structure is more regularly and orderly.

XRD analysis of Na-bentonite shows that the main peaks (montmorillonite) are correspondence to the crystal structure of bentonite. The other peaks correspond to the impurities of feldspar, quartz and Fe(Ca)CO3.

Speciation is one of the most important factors influencing the sorption of Am (III) on bentonite. There are at least 4 speciation in aqueous solution: $Am^{3+}$, $Am(OH)^{2+}$, $Am(OH)_2^+$ and $Am(OH)_3$. At *p*H

Table 1 — Linear and non-linear forms of pseudo-first-order, pseudo-second-order kinetics models

| Type | Nonlinear form | Linear form | Plot | Parameters |
|---|---|---|---|---|
| 1 | $q_t=q_e(1-e^{-K_1t})$ | $\ln(q_e-q_t)=\ln q_e-K_1t$ | *ln($q_e$-$q_t$)* vs. *t* | $q_e$=exp(*intercept*)<br>$K_1$=- *slope* |
| 2 | $q_t=\frac{K_2q_e^2t}{1+K_2q_et}$ | $\frac{t}{q_t}=\frac{1}{K_2q_e^2}+\frac{1}{q_e}t$ | *t*/$q_t$ vs. *t* | $q_e$=1/*slope*<br>$K_2$=*slope*$^2$/*intercept* |
| 3 | | $\frac{1}{q_t}=\frac{1}{q_e}+\frac{1}{K_2q_e^2}\frac{1}{t}$ | 1/$q_t$ vs. 1/*t* | $q_e$=1/*intercept*<br>$K_2$=*intercept*$^2$/*slope* |
| 4 | | $q_t=q_e-\frac{1}{K_2q_e}\frac{q_t}{t}$ | $q_t$ vs. $q_t$/*t* | $q_e$=*intercept*<br>$K_2$=−1/(*intercept*×*slope*) |
| 5 | | $\frac{q_t}{t}=K_2q_e^2-K_2q_eq_t$ | $q_t$/*t* vs. $q_t$ | $q_e$= −*intercept*/*slope*<br>$K_2$=*slope*$^2$/*intercept* |

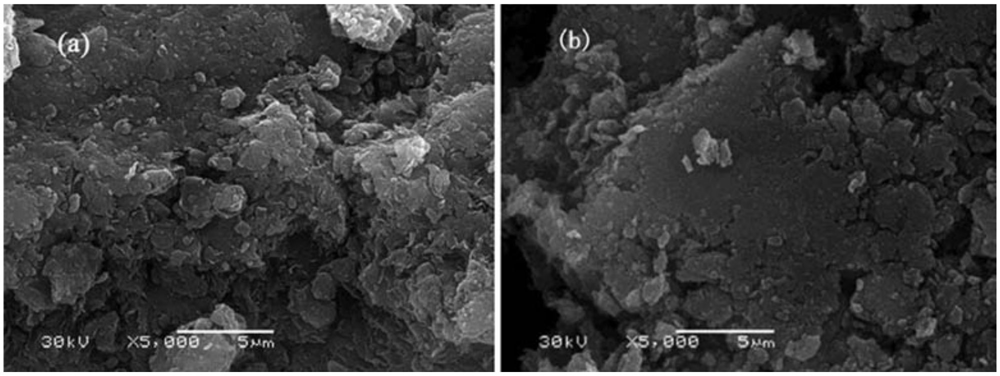

Fig. 1 — SEM micrographs of raw bentonite(a) and Na-bentonite(b).

>4, the hydrolysis occurs for Am(III); *p*H <5, $Am^{3+}$ is dominant(>90%); *p*H = 6, $Am^{3+}$ and $Am(OH)^{2+}$ are about 50%, respectively; $Am(OH)_2^+$ is the main speciation in the range of *p*H 8-12; *p*H >12, the dominant speciation is $Am(OH)_3$ [24].

**Effect of solid content (m/V)**

The sorption of Am (III) on Na-bentonite as a function of solid content is shown in Fig. 2, the curve of $\ln K_d$ is shown in Fig. 2 as well. With the increase of bentonite content, the sorption percentage of Am (III) increases, indicates that the functional groups to bind Am (III) at each bentonite surface increase, more sites on bentonite surfaces are provided to adsorb metal ions. The values of $\ln K_d$ increase a little with increasing bentonite contents shows that the distribution of Am (III) trend to equilibrium between solid phase and liquid phase, and more sorption sites could not increase the distribution obviously at $m/V$>0.1g/L [25].

**Sorption kinetics**

The sorption of Am (III) on Na-bentonite as a function of contact time was investigated. As can be seen in Fig. 3(a), the sorption of Am (III) is very quick and about 4 h are enough to achieve the sorption equilibrium; after 4 h, the removal percent maintained a constant level and independent of contacted time. One phenomenon worthy of note is that a little decrease appears before the sorption achieved equilibrium, which indicates that sorption of Am (III) on bentonite is mainly attributed to physical sorption rather than chemical sorption in initial 4 h, however the chemical sorption dominates in the following time. Twelve hours is selected as contact time in the following experiments. With the temperature increased, the sorption percentage and sorption velocity were all increased.

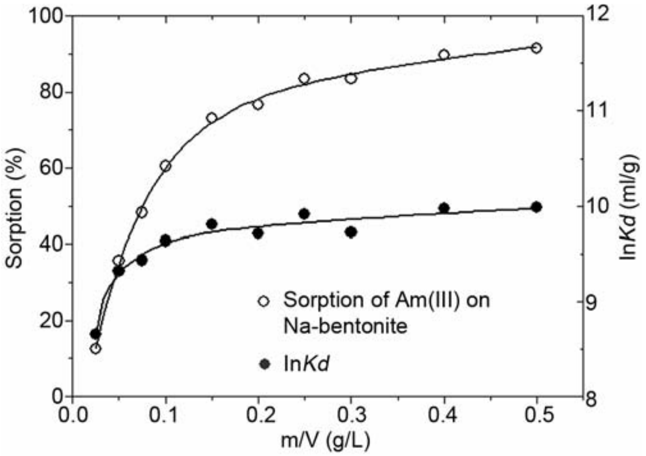

Fig. 2 — Sorption of Am (III) on Na-bentonite as a function of solid content: T = 298.15K, *p*H = 3.50, $C_{Am(III)initial} = 3.6\times10^{-9}$mol/L , I = 0.05mol/L NaCl.

The sorption of Am (III) on Na-bentonite and the non-linear and linear fitting curves of sorption kinetics are shown in Fig. 3. Figure 3(a) shows the sorption is mainly attributed to physical sorption rather than chemical sorption in initial 4h for the increase-decrease progress before the sorption achieved equilibrium, and the sorption percentage maintains a constant level and independent of contacted time after 4 h. Twelve hours are selected as contact time in the next experiments. Through duplicate experiments of every site in Fig. 3(a), the overall experimental error is less than 5%.

The non-linear fitting curves of pseudo-first-order, pseudo-second-order and pseudo-n-order kinetic equations are shown in Fig. 3(b). The result shows that the three curves could fit the experimental data well and it can not be estimated which is the best method among the three equations. Figures 3(c) and 3(d) show the linear plot feature of $\ln(q_e\text{-}q_t)$vs. $t$, $t/q_t$ vs.$t$ at different temperatures (type 1, 2) are achieved, from these figures, one can see that pseudo-second-

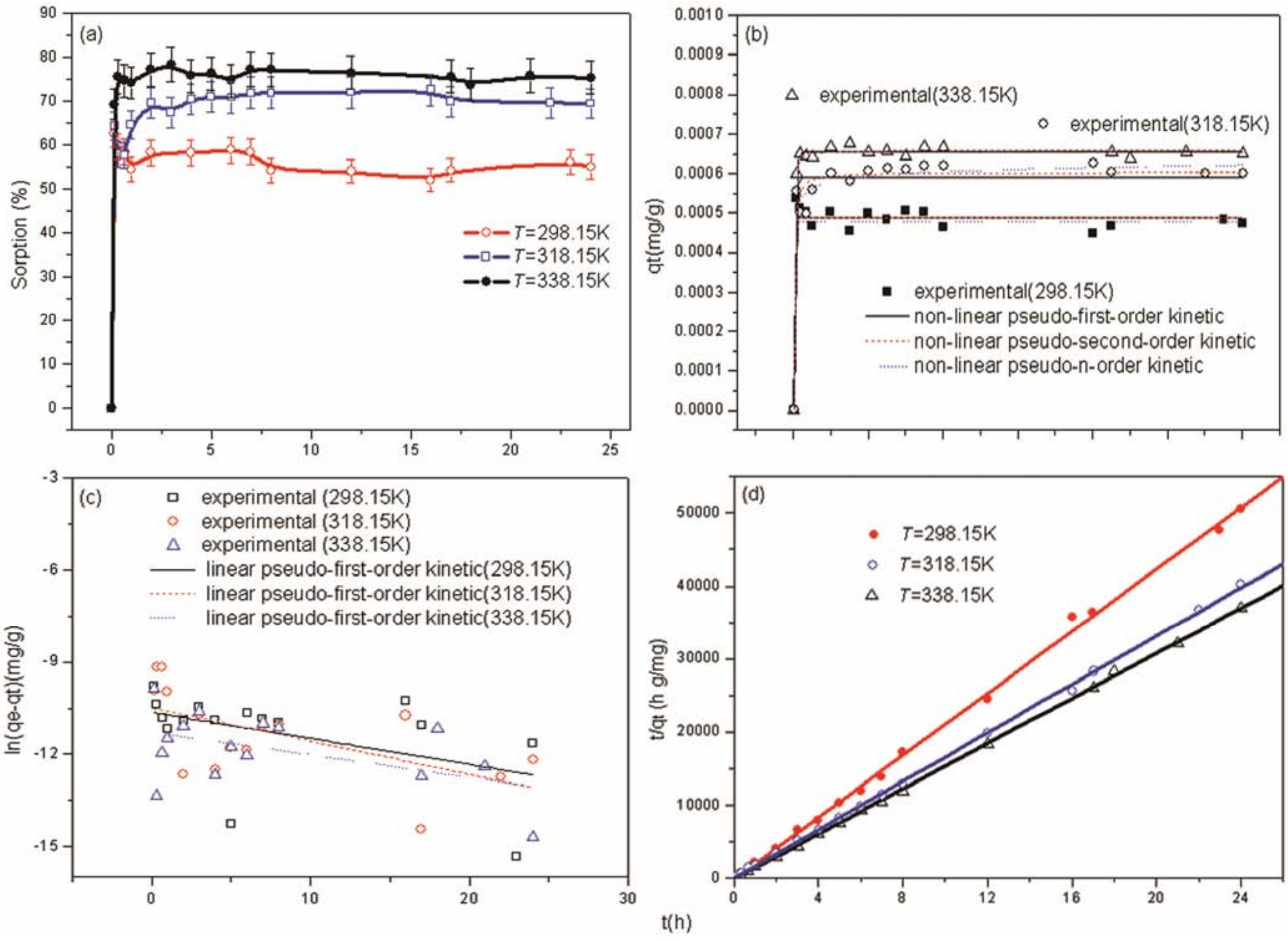

Fig. 3 — Sorption of Am (III) as a function of contact time. I = 0.05 mol/L NaCl, m/V = 0.1g/L.

order kinetic equation fits the experimental data better than pseudo-first-order by linear method.

The parameters of the three kinetic equations by non-linear and linear method at 298.15K, 318.15K and 338.15K are listed in Table 2. The linear forms of type 3, 4, 5 in Table 1 were drawn as well and the results indicated that the linearity of the three types to the experimental data are very weak. From Table 2, the values of $q_e$ of the three types (type 1, 2 and Equation 15) and two methods (linear and non-linear method) are different, while the values of $K_1$, $K_2$ and $K_n$ vary widely. To the three types, the relatively lower $x^2$ and higher $R^2$ values of the pseudo-second-order expression shows that compared to the other expressions, the linear and non-linear pseudo-second-order kinetic equation could fit the kinetics of Am (III) on Na-bentonite better than the other ones. To the two methods, the relatively lower $x^2$ of non-linear method suggest the non-linear method is the better way to describe the sorption kinetics. These results indicate that the non-linear pseudo-second-order may be the best method to express the sorption kinetics in this sorption system.

The negative value of $K_2$ by linear method indicated that the sorption is the dominant reaction rather than desorption in the initial stage, while desorption become the dominant reaction gradually with contact time increasing, and the sorption percentage shows a decline result. With the increase of temperature, the values of $K_2$ by non-linear method increase, too. This shows that sorption speed is faster at higher temperature [26].In order to obtain better understanding of the rate controlling factors that affect the kinetics of sorption, the diffusion model and Weber-Morris intraparticle diffusion model were used to simulate the experimental data. The linear plot feature of $-ln(1-F)$-0.4977 vs. $t$ at different temperatures are achieved, and shown in Fig. 4. Figure 4 shows the fitting curves of sorption diffution model at different temperatures. From Fig. 4, it is

Table 2 — Linear and non-linear methods' pseudo-first-order(1), pseudo-second-order(2) and pseudo-n-order(3) kinetic parameters for sorption of Am (III) on Na-bentonite

| Type | $q_e$(mg/g) | | | | | | $K$ | | | | | |
|---|---|---|---|---|---|---|---|---|---|---|---|---|
| | 298.15K | | 318.15K | | 338.15K | | 298.15K | | 318.15K | | 338.15K | |
| | Linear method | Non-linear method | Linear method | Non-linear method | Linear method | Non-linear method | Linear method | Non-linear method | Linear method | Non-linear method | Linear method | Non-linear method |
| 1 | $2.394\times10^{-5}$ | $4.876\times10^{-4}$ | $2.781\times10^{-5}$ | $5.886\times10^{-4}$ | $1.262\times10^{-5}$ | $6.533\times10^{-4}$ | 0.0846 | 1098 | 0.1082 | 14.81 | 0.0739 | 14.66 |
| 2 | $4.711\times10^{-4}$ | $4.876\times10^{-4}$ | $6.044\times10^{-4}$ | $6.015\times10^{-4}$ | $6.468\times10^{-4}$ | $6.568\times10^{-4}$ | $3.168\times10^{4}$ | $4.707\times10^{4}$ | $2.213\times10^{5}$ | $4.830\times10^{4}$ | $3.278\times10^{4}$ | $1.111\times10^{5}$ |
| 3 | n=1.158, $q_e$=$4.776\times10^{-4}$ | | n=5.886, $q_e$=$6.803\times10^{-4}$ | | n=0.9977, $q_e$=$6.532\times10^{-4}$ | | - | $9.161\times10^{4}$ | - | $3.196\times10^{18}$ | - | 14.38 |
| Type | $x^2$ | | | | | | $R^2$ | | | | | |
| | 298.15K | | 318.15K | | 338.15K | | 298.15K | | 318.15K | | 338.15K | |
| | Linear method | Non-linear method | Linear method | Non-linear method | Linear method | Non-linear method | Linear method | Non-linear method | Linear method | Non-linear method | Linear method | Non-linear method |
| 1 | $1.350\times10^{-1}$ | $1.767\times10^{-5}$ | $1.683\times10^{-1}$ | $4.522\times10^{-5}$ | $4.819\times10^{-1}$ | $7.519\times10^{-6}$ | 0.1551 | 0.9601 | 0.3042 | 0.9318 | 0.1927 | 0.9956 |
| 2 | $2.693\times10^{-5}$ | $1.767\times10^{-5}$ | $5.695\times10^{-5}$ | $5.383\times10^{-5}$ | $7.319\times10^{-6}$ | $8.425\times10^{-6}$ | 0.9992 | 0.9601 | 0.9994 | 0.9579 | 0.9997 | 0.9946 |
| 3 | - | $2.116\times10^{-5}$ | - | $2.926\times10^{-4}$ | - | $7.502\times10^{-6}$ | - | 0.9496 | - | 0.9707 | - | 0.9953 |

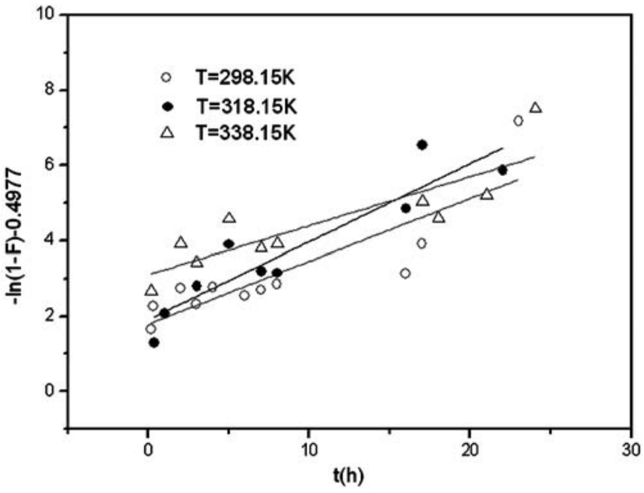

Fig. 4 — Fitting curves of diffusion kinetic model for Am (III) sorption onto Na-bentonite. $p$H = 3.0, I = 0.05 mol/L NaCl, m/V = 0.1g/L.

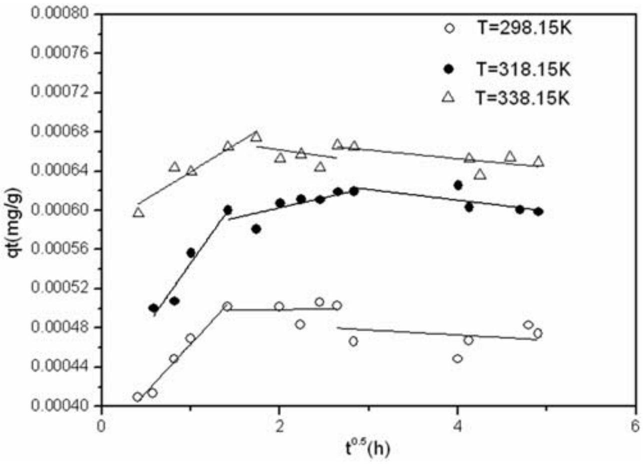

Fig. 5 — Fitting curves of Weber-Morris intraparticle diffusion model for Am (III) sorption onto Na-bentonite. $p$H = 3.0, I = 0.05 mol/L NaCl, m/V = 0.1g/L.

shown that the plots close to the origin but do not pass through it. This indicates that the process of sorption is very complex, and the diffusion is an important control process and involved in the sorption process.

The fitting curves of Weber-Morris intraparticle diffusion model at different temperatures are shown in Fig. 5, and the parameters mentioned above are listed in Table 3. From Fig. 5, it is can be seen that intraparticle diffusion of Am(III) sorption onto Na-bentonite occurs in three stages: An initial curve portion; A buffer portion; An equilibrium portion. The first curve portion is ascribed to the diffusion of adsorbate through the solution to the surface of Na-bentonite or diffusion of solute molecules; The second portion suggests the gradual sorption stage, where the intraparticle diffusion was rate limiting;

While the third portion is the equilibrium stage. The plots also show that the intraparticle diffusion is not the only controlling step and the sorption mechanism is very complex.

The parameters listed in Table 3 shows that the diffusion rate at 318.15K is faster than it at 298.15K and 338.15K according to the $k_p$ values. The result indicates that the rate of diffusion is most affected at moderate temperature. The influence of boundary layer can not be ignored and it increases with the increase of temperature according to the values of C.

**Effect of *p*H and ionic strength**

Figure 6 shows a 3D image of the Am (III) distribution ($C_s$-$C_{eq}$) as a function of *p*H value in 0.01, 0.05 and 0.1M NaCl solutions, respectively. From Fig.6, the removal of Am (III) is strongly dependent on *p*H values and ionic strength. Sorption percent of Am (III) increased from 0 to 95% with the increasing of *p*H values from 1 to 2.5 in 0.01M NaCl solution, and then maintains the high level with further increasing *p*H values before *p*H = 7. However, the sorption percent drops down to 70% from *p*H 7 to *p*H 12. In 0.1M NaCl solution, the sorption percent increases from 0 to 95% with the increase of *p*H values from 3.1 to 7, while maintains the high level with further increasing *p*H values. At *p*H <7, the removal of Am (III) in 0.01M NaCl solution is much higher than that of Am (III) in 0.05M and 0.1M NaCl solution. This shows that the sorption of Am (III) on bentonite is strongly affected by ionic strength [27].

Table 3 — Parameters of Weber-Morris intraparticle diffusion model for sorption of Am (III) on Na-bentonite

| *T*/K | $k_p$/g/(mg h$^{0.5}$) | *C*/mg/g | $R^2$ |
|---|---|---|---|
| 298.15 | $9.823\times10^{-5}$ | $3.655\times10^{-4}$ | 0.9717 |
| 318.15 | $1.285\times10^{-4}$ | $4.182\times10^{-4}$ | 0.9068 |
| 338.15 | $5.575\times10^{-5}$ | $5.833\times10^{-4}$ | 0.8791 |

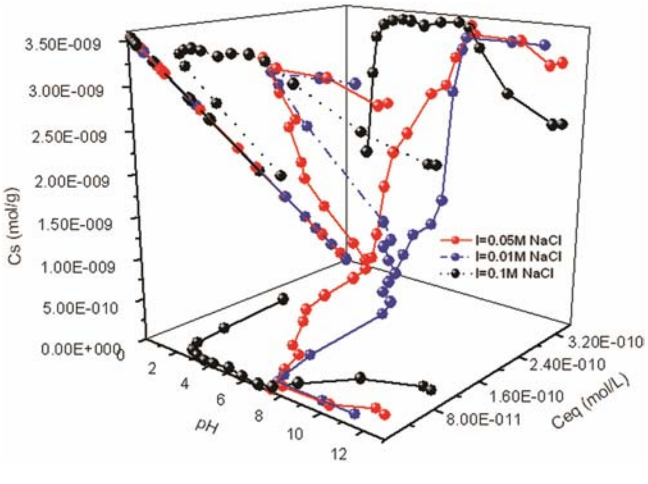

Fig. 6 — Sorption of Am (III) on bentonite as a function of *p*H and ionic strength. $c_{(Am)0}$ = $0.36\times10^{-9}$mol/L, *T* = 298.15K, m/V = 0.1g/L.

Removal percent of Am (III) from solution to bentonite as a function of *p*H in different ions background electrolyte solutions was investigated. The results show that LiCl has a little influence to the sorption of the system, compared to NaCl in the same concentration, while the negative influence of KCl is more significantly, the influence of $K^+$ ions on the sorption of Am (III) indicated that ion exchange or outer-sphere complexes may be formed on bentonite at low *p*H. The influence of negative ions shows the same characteristic that monoacidic ions have little influence to the sorption, such as $Cl^{-1}$ and $NO_3^{-1}$. The inner-sphere complexes are formed at high *p*H. These results suggest that surface complexation is obviously influenced by *p*H values, and ion exchange is influenced by ionic strength [28].

According to the experimental results, the sorption mechanism of Am (III) is assumed: the solid surface is assumed to be both permanent negative charge site (=XNa) which originates from isomorphous replacement and a number of variable charge sites (=S–OH) which could be either protonated and deprotonated. The sorption mechanism of Am (III) on Na-bentonite can be presumed by following reactions[14]:

***i) ion exchange:***

$$=XNa+Am^{3+} \Leftrightarrow XAm^{2+} + Na^+ \quad \ldots (19)$$

$$2=XNa+Am^{3+} \Leftrightarrow X_2\,Am^+ + 2Na^+ \quad \ldots (20)$$

$$3=XNa+Am^{3+} \Leftrightarrow X_3\,Am + 3Na^+ \quad \ldots (21)$$

***ii) sorption and hydrolysis at the surface of the Na-bentonite:***

$$(=S\text{-}OH)+H_2O+Am^{3+} \Leftrightarrow (S\text{-})Am(OH)_2^{2+}+H^+ \quad \ldots (22)$$

$$(=S\text{-}OH)+2H_2O+Am^{3+} \Leftrightarrow (S\text{-})Am(OH)_3^{+}+2H^+ \quad \ldots (23)$$

$$(=S\text{-}OH)+3H_2O+Am^{3+} \Leftrightarrow (S\text{-})Am(OH)_4 +3H^+ \quad \ldots (24)$$

***iii) hydrolysis of $Am^{3+}$ in solution:***

$$Am^{3+} + nH_2O \Leftrightarrow [Am(OH)_m\,(H_2O)_{n-m}\,]^{3-m} +mH^+ \quad \ldots (25)$$

being n > m, and exchange with hydrolyzed species:

$$(=S\text{-}OH)+ \ [Am(OH)_m \ (H_2O)_{n-m} \ ]^{3-m} \Leftrightarrow (S\text{-}O)\text{-}Am(OH)_m^{2-m} + H^+ +(n\text{-}m)\,H_2O \quad \ldots (26)$$

### Effect of humic acid

The influence of humic acid on Am (III) sorption onto Na-bentonite at various *p*H was studied. The results indicate that at $c_{HA}$ = 5mg/L, the presence of HA enhances the sorption of Am (III) on HA-bentonite hybrids obviously at *p*H <6, reduces the sorption at *p*H >6; At $c_{HA}$=10mg/L, the presence of HA enhances the sorption at *p*H <4, and reduces the sorption at *p*H >4. The increase of Am (III) sorption on HA–bentonite hybrids in low *p*H range may be attributed to a reduction in positive surface charge caused by the sorption of negatively charged HA at bentonite surfaces, which resulted in a more favorable electrostatic environment for Am (III) sorption and enhances the formation of ternary Am–HA-bentonite surface complexes[4]. The negative effect of HA at *p*H >6 and *p*H >4 are attributed to the strong soluble complexes of HA–Am (III) in solution, respectively. At *p*H 7, both of the two lines show a peak valley, as the surface charge of bentonite is negative and the sorption of negatively charged HA on the negatively charged bentonite surface decreases with increasing *p*H due to electrostatic repulsion. At *p*H >7, both of the lines increased to a certain extent again, as the physical sorption plays a main role.

The solid surface contains a number of variable charge sites (=SO-H) which could be either protonated and deprotonated. The sorption mechanism of Am (III) on Na-bentonite in the presence of HA could be postulated by following reactions:

$$(=S\text{-}OH)+HA\text{-}COOH+Am^{3+}\Leftrightarrow(=S\text{-}O)\text{-}OC\text{-}HA\text{-}Am^{3+}+H_2O \quad \ldots (27)$$

$$(=S\text{-}O)\text{-}OC\text{-}HA\text{-}Am^{3+}+H_2O\Leftrightarrow(=S\text{-}OH)+HA\text{-}COOH+Am^{3+} \quad \ldots (28)$$

$$(=S\text{-}O)\text{-}Am^{3+}+HA\text{-}COOH\Leftrightarrow(=S\text{-}OH)+HA\text{-}COO\text{-}Am^{3+} \quad \ldots (29)$$

### Sorption isotherms

There are several linear and non-linear sorption models could describe the sorption isotherm of Am (III) onto Na-bentonite. Furthermore, these models have different number of parameters such as two-parameter models, Langmuir and Freundlich model, and three-parameter models, Sips and Toth model. These models were adopted to express the isotherms of the sorption as a function of temperature in order to represent the sorption mechanism. Models mentioned above are described in Table 4[29-31].

$C_s$ (mol/g) is the equilibrium sorption capacity, $C_{eq}$ (mol/L) is the concentration of Am (III) in liquid phase, $C_{max}$ (mol/g) is the maximum sorption capacity, *b* is a constant that relates to the heat of sorption, *a* and *n* are constants.

#### *Sorption isotherms by linear method*

Langmuir and Freundlich linear models are the commonly used linear sorption isotherm. Meanwhile, Langmuir isotherm is transformed to at least four linear forms. The parameters of Langmuir and Freundlich models mentioned above have been

Table 4 — Sorption isotherms in linear or non-linear forms

| Isotherms | Nonlinear | Linear | Plot | Parameters |
|---|---|---|---|---|
| Langmuir 1 | $c_s=\frac{bc_{max}c_{eq}}{1+bc_{eq}}$ | $\frac{c_{eq}}{c_s}=\frac{1}{bc_{\max}}+\frac{c_{eq}}{c_{\max}}$ | $\frac{c_{eq}}{c_s}$ *vs.* $c_{eq}$ | *b=slope/intercept*<br>$c_{max}$*=1/slope* |
| Langmuir 2 | | $\frac{1}{c_s}=(\frac{1}{bc_{\max}})\frac{1}{c_{eq}}+\frac{1}{c_{\max}}$ | $\frac{1}{c_s}$ *vs.* $\frac{1}{c_{eq}}$ | *b=intercept/slope*<br>$c_{max}$*=1/ intercept* |
| Langmuir 3 | | $c_s=c_{\max}-(\frac{1}{b})\frac{c_s}{c_{eq}}$ | $c_s$ *vs.* $\frac{c_s}{c_{eq}}$ | *b=-1/slope*<br>$c_{max}$*=intercept* |
| Langmuir 4 | | $\frac{c_s}{c_{eq}}=bc_{\max}-bc_s$ | $\frac{c_s}{c_{eq}}$ *vs.* $c_s$ | *b=-slope*<br>$c_{max}$*=-intercept/slope* |
| Freundlich | $c_s=ac_{eq}{}^n$ | $\lg c_s=\lg a+n\lg c_{eq}$ | $lgc_s$ *vs.* $lgc_{eq}$ | *a= exp(intercept)*<br>*n=slope* |
| Sips | $c_s=\frac{c_{\max}(bc_{eq})^n}{1+bc_{eq}}$ | | | |
| Toth | $q_e=\frac{c_{\max}bc_{eq}}{(1+(bc_{eq})^n)^{1/n}}$ | | | |

plotted in Fig. 7. The parameters have been calculated and listed in Table 5. Langmuir 2-4 models are not drawn because of their weak linearity. From Fig. 7 and Table 5, one can see the values of $R^2$of Freundlich model are higher than them of Langmuir model in general. Moreover, the parameters of Langmuir model appear manifest errors for the negative values. The results indicate that the Freundlich model fit to describe the sorption process better than the Langmuir model by linear method.

From Fig. 7(b), with the increase of temperature, the values of $K_d$ increase, and Am (III) migrates to the absorbent as well. The thermodynamic parameters ($\Delta G^{\circ}$, $\Delta S^{\circ}$, and $\Delta H^{\circ}$) for Am (III) sorption on Na-bentonite can be calculated from the equations [4, 22]:

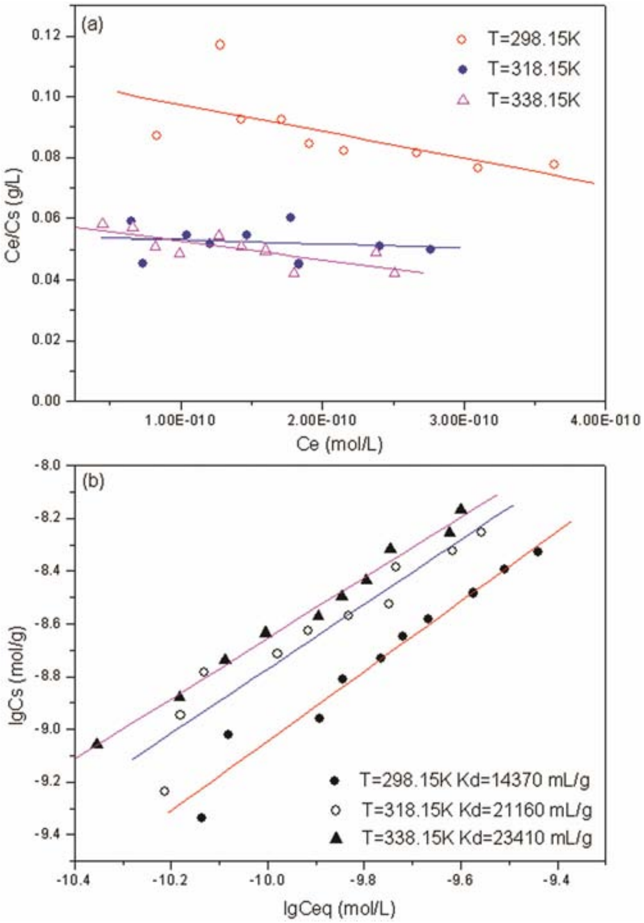

Fig. 7 — Linear Langmuir (a) and Freundlich (b) isotherms for Am (III) sorption on Na-bentonite. *p*H = 3.0, m/V = 0.1g/L, I = 0.05 mol/L NaCl.

$$\Delta G^0 = -RT \ln K_d \qquad \dots (30)$$

$$\left(\frac{\partial G^0}{\partial T}\right)_p = -\Delta S^0 \qquad \dots (31)$$

$$\Delta H\mathrm{p} = \Delta G^0 + T\Delta S^0 \qquad \dots (32)$$

where $R$ (8.3145 J mol$^{-1}$ K$^{-1}$) is the ideal gas constant, and $T$(K) is the temperature in Kelvin. The values mentioned above are tabulated in Table 6.

The values of standard enthalpy change (ΔH°) are positive value, which indicates that the holistic sorption process is endothermic. Under the conditions applied, the sorption is a spontaneous process, as the Gibbs free energy changes (ΔG°) are negative. With the increase of temperature, the value of ΔG° become more negative, and more efficient sorption at high temperature as expected. At high temperature, cations are readily desolvated and hence their sorption becomes more favorable[32]. The positive values of entropy change (ΔS°) reflect the affinity of Na-bentonite toward Am (III) ions in aqueous solutions and may suggest some structure changes on the adsorbents [33].

### *Sorption isotherms by non-linear method*

The four sorption isotherms mentioned above (Langmuir, Freunlich, Sips and Toth) at different temperatures by non-linear method are drawn in Fig. 8, and the isotherm parameters are calculated and listed in Table 7, respectively. To two parameters models (Langmuir1 and Freundlich), from Table 7, it is observed that Freundlich model fits the sorption better because it's higher $R^2$ and lower $x^2$ at the three temperatures. To three parameters models (Sips and Toth), Sips model could fit the sorption better because it's higher $R^2$ and lower $x^2$ at every temperature. There is a notable phenomenon that the '*n*' values of Freundlich and Sips model are the same because the similar expressions of the two isotherm models. Compare to three parameters models, two parameters models fit the sorption better, as a whole. This

Table 5 — Parameters of Langmuir, Freundlich isotherms by linear method

| *T*/K | Langmuir 1 | | | Freundlich | | |
|---|---|---|---|---|---|---|
| | $c_{max}$ | *b* | $R^2$ | *a* | *n* | $R^2$ |
| 298.15 | -5.690×10$^{-9}$ | -1.360×10$^{9}$ | 0.3698 | 66.97 | 1.325 | 0.9539 |
| 318.15 | -9.864×10$^{-9}$ | -1.403×10$^{9}$ | 0.0797 | 32.46 | 1.225 | 0.8929 |
| 338.15 | -16.60×10$^{-9}$ | -1.017×10$^{9}$ | -0.5693 | 16.24 | 1.151 | 0.9888 |

Table 6 — Values of thermodynamic parameters for Am (III) sorption on Na-bentonite

| T(K) | $\Delta G^0$(kJ mol$^{-1}$) | $\Delta S^0$ (J K$^{-1}$ mol$^{-1}$) | $\Delta H^0$ (kJ mol$^{-1}$) |
|---|---|---|---|
| 298.15 | -23.73 | 113.9 | 10.23 |
| 318.15 | -26.34 | 113.9 | 9.892 |
| 338.15 | -28.29 | 113.9 | 10.23 |

Table 7 – Isotherm parameters for Am(III) sorption on Na-bentonite by non-linear method

| T/K | Langmuir 1 | | | | Freundlich | | | |
|---|---|---|---|---|---|---|---|---|
| | $c_{max}$ | $b$ | $R^2$ | $x^2$ | $a$ | $n$ | $R^2$ | $x^2$ |
| 298.15 | 0.1105 | 110.5 | 0.958 | $8.038\times10^{-20}$ | 2208 | 1.236 | 0.9888 | $2.150\times10^{-20}$ |
| 318.15 | 0.1395 | 139.4 | 0.9502 | $1.280\times10^{-19}$ | 204.2 | 1.105 | 0.9575 | $1.092\times10^{-19}$ |
| 338.15 | 0.1464 | 144.3 | 0.9602 | $1.089\times10^{-19}$ | 838.2 | 1.164 | 0.9756 | $6.627\times10^{-20}$ |

| T/K | Sips | | | | | Toth | | | | |
|---|---|---|---|---|---|---|---|---|---|---|
| | $c_{max}$ | $b$ | $n$ | $R^2$ | $x^2$ | $c_{max}$ | $b$ | $n$ | $R^2$ | $x^2$ |
| 298.15 | 2.519 | 240.9 | 1.236 | 0.9872 | $2.457\times10^{-20}$ | 5.180 | 2.353 | 1.696 | 0.952 | $9.187\times10^{-20}$ |
| 318.15 | 1.122 | 111.0 | 1.105 | 0.9514 | $1.248\times10^{-19}$ | 8.820 | 2.205 | 9.923 | 0.9431 | $1.463\times10^{-19}$ |
| 338.15 | 1.967 | 181.5 | 1.164 | 0.9722 | $7.574\times10^{-20}$ | 9.193 | 2.298 | 4.576 | 0.9545 | $1.238\times10^{-19}$ |

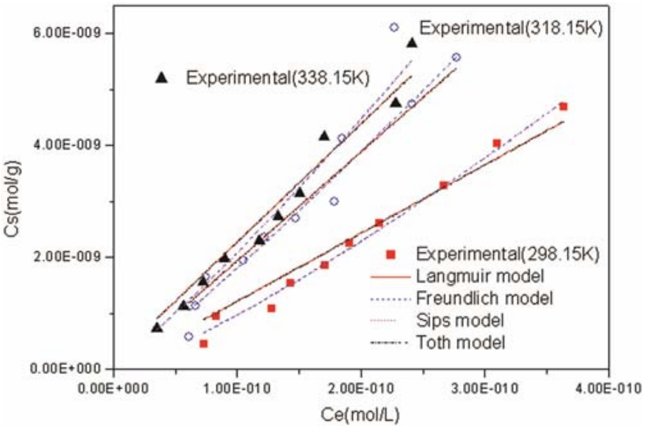

Fig. 8 — Non-linear isotherms of Am (III) sorption on Na-bentonite as a function of temperature. *p*H = 3.0, m/V = 0.5g/L, I = 0.05 mol/L NaCl.

indicates the congenital advantage of the nonlinear method over the linear method. These results could be accounted for by the differences in efficiency of an iterative procedure employed in a nonlinear method and the restrictions of a linear regression[13].

From Fig. 8, it shows that the fitting curves of Langmuir and Freundlich models are very close at different temperatures, and the Frundlich and Sips, Langmuir and Toth models' fitted curves are almost overlap at the three temperatures. These may be because Langmuir and Freundlich models fit the sorption in the similar degree, and Freundlich and Sips, Langmuir and Toth models have the similar expressions. Combined with the results mentioned above (Table 7), the results indicated that the sorption process could not describe by mono molecule layer sorption model, and the physicochemical behaviour of Am (III) is dominated by many factors.

## Conclusion

From the results of Am (III) sorption on Na-bentonite at different experimental conditions, the following conclusions can be drawn:

(1) Sorption of Am (III) on Na-bentonite is strongly dependent on *p*H values and ionic strength. Surface complexation and ion exchange assumes to explain the sorption mechanism of Am (III) at high or low *p*H range.

(2) The kinetic sorption of Am (III) on bentonite could be described well by a linear pseudo-second-order model, and the non-linear pseudo-second-order kinetic expression could fit the kinetics better, compared to the linear forms.

(3) The presence of different foreign univalent cations and anions has no obvious influence on the sorption of Am (III) on Na-bentonite. The presence of HA enhances the sorption of Am (III) on Na-bentonite at low *p*H values.

(4) The sorption of Am (III) on Na-bentonite is an endothermic and spontaneous process, indicated by the thermodynamic parameters.

(5) Two-parameter models and three-parameter models were adopted to simulate the sorption thermodynamics processes, and Freundlich isotherm model is the best-fit model to the experimental data for the sorption of Am (III) on Na-bentonite. Non-linear method is a better way to represent the sorption isotherms than the linear method. Non-linear method was found to be the

more appropriate method to determine kinetic and thermodynamic parameters in this experimental system.

## Acknowledgement

Financial support from National Natural Science Foundation of China (21561001), the project supported by Natural Science Foundation of Jiangxi, China (20161BAB203100), and Science and Technology Research Project of Jiangxi Provincial Education Development (GJJ13454) are acknowledged.

## References

1 Das D K, Pathak P N, Kuma R S & Manchanda V K, *J Radioanal Nucl Ch*, 281 (2009) 449.
2 Rabung Th, Stumpf Th, Geckeis H, Klenze R & Kim J I, *Radiochim Acta*, 88 (2000) 711.
3 Wanner H, Albinsson Y & Wieland E, *Fresen J Anal Chem*, 354 (1996)763.
4 Yang S T, Li J X, Lu Y, Chen Y X & Wang X K, *Appl Radiat Isotopes*, 67 (2009) 1600.
5 Hu J, Xie Z, He B, Sheng G D, Chen C L, Li J X, Chen Y X & Wang X K, *Sci China Chem*, 53 (2010) 1420.
6 Ye W M, Wan M, Chen B, Chen Y G, Cui Y J & Wang J, *J Cen. South Univ T,* 16 (2009) 821.
7 Mirashi N N, Shan P M & Aggarwal S K, *J Radioanal Nucl Chem*, 275 (2008) 479.
8 Ivanova Ju, Djingova R & Kuleff I, *J Radioanal Nucl Ch*, 238 (1998) 29.
9 Ho Y S, *Pol J Environ Stud*, 15 (2006) 81.
10 Sari A & Tuzen M, *J Hazard Mater*, 160 (2008) 349.
11 Prasad M & Saxena S, *Ind Eng Chem Res*, 43 (2004)1512.
12 Yu T, Wu W S, Liu Z R, Zhang S W & Nie Z W, *Korean J Chem Eng,* 30 (2013) 440.
13 Parimal S, Prasad M & Bhaskar U, *Ind Eng Chem Res*, 49 (2010) 2882.
14 Yu T, Wu W S & Fan Q H, *Chinese Chem Lett*, 23 (2012) 1189.
15 Guo Z J, Xu J, Shi K L, Tang Y Q, Wu W S & Tao Z Y, *Colloid Surface A*, 339 (2009) 126.
16 Fan Q H, Xu J Z, Niu Z W, Li P & Wu W S, *Appl Radiat Isotopes*, 70 (2012) 13.
17 Vadivelan V & Kumar K Vasanth, *J Colloid Interf Sci*, 286 (2005) 90.
18 Chowdhury S & Das P, *Bioremediat J*, 15 (2011) 99.
19 Kumar K Vasanth, *J Hazard Mater*, B137 (2006) 1538.
20 Chowdhury S & Saha P, *Bioremediat J*, 14 (2010) 196.
21 Kumar K Vasanth & Sivanesan S, *J Hazard Mater*, 134 (2006) 237.
22 Aksu Z, *Process Biochem*, 40 (2005) 997.
23 Zhang J Y, Wu C D, Jia A Y & Hu B, *Appl Surf Sci,* 298 (2014) 95.
24 Fan Q H, Zhang M L, Zhang Y Y, Ding K F, Yang Z Q & Wu W S, *Radiochim Acta*, 98 (2010) 19.
25 Murali M S & Mathur J N, *J Radioanal Nucl Ch,* 254 (2002) 129.
26 Evans N, Warwick P, Lewis T & Beyan N, *Environ Chem Lett*, 9 (2011) 25.
27 Akşay H, *J Radioanal Nucl Ch*, 237 (1998) 133.
28 Palágyi Š, Vodičková H, Landa J, Palágyiová J & Laciok A, *J Radioanal Nucl Ch*, 279 (2009) 431.
29 Chowdhury S, Mishra R, Kushwaha P & Das P, *Bioremed J*, 15 (2011)77.
30 Belhachemi M & Addoun F, *Appl Water Sci*, 1 (2011) 111.
31 Terzyk A P, Chatlas J, Gauden P A, Rychlick G & Kowalczyk P, *J Colloid Interf Sci*, 266 (2003) 473.
32 Fan Q H, Shao D D, Lu Y, Wu W S & Wang X K, *Chem Eng J,* 150 (2009) 188.
33 Humelnicu D, Drochioiu G, Sturza M I, Cecal A & Popa K, *J Radioanal Nucl Ch*, 270 (2006) 637.